Supporting Information for "Future trends of agricultural ammonia global emissions in a changing climate"

M Beaudor[1,2], N Vuichard[1], J Lathiere[1], D Hauglustaine[1]

[1]Laboratoire des Sciences du Climat et de l'Environnement (LSCE) CEA-CNRS-UVSQ, Gif-sur-Yvette, France

[2]The High Meadows Environmental Institute, Princeton University, Princeton, 08540, NJ, USA

Contents of this file Figures S1 to S10

References

Beaudor, M., Vuichard, N., Lathière, J., Evangeliou, N., Van Damme, M., Clarisse, L., & Hauglustaine, D. (2023, February). Global agricultural ammonia emissions simulated with the ORCHIDEE land surface model. *Geoscientific Model Development*, *16*(3), 1053–1081. Retrieved 2023-05-12, from https://gmd.copernicus.org/articles/16/1053/2023/ (Publisher: Copernicus GmbH) doi: 10.5194/gmd-16-1053-2023

Hoesly, R. M., Smith, S. J., Feng, L., Klimont, Z., Janssens-Maenhout, G., Pitkanen, T., ... Zhang, Q. (2018, January). Historical (1750–2014) anthropogenic emissions of reactive gases and aerosols from the Community Emissions Data System (CEDS). *Geoscientific Model Development*, *11*(1), 369–408. Retrieved 2021-08-26, from https://gmd.copernicus.org/articles/11/369/2018/ (Publisher: Copernicus GmbH) doi: 10.5194/gmd-11-369-2018

Riahi, K., van Vuuren, D. P., Kriegler, E., Edmonds, J., O'Neill, B. C., Fujimori, S., ... Tavoni, M. (2017, January). The Shared Socioeconomic Pathways and their energy, land use, and greenhouse gas emissions implications: An overview. *Global Environmental Change*, *42*, 153–168. Retrieved 2022-02-11, from https://linkinghub.elsevier.com/retrieve/pii/S0959378016300681 doi: 10.1016/j.gloenvcha.2016.05.009

van der Werf, G. R., Randerson, J. T., Giglio, L., van Leeuwen, T. T., Chen, Y., Rogers, B. M., ... Kasibhatla, P. S. (2017, September). Global fire emissions estimates during 1997–2016. *Earth System Science Data*, *9*(2), 697–720. Retrieved 2022-07-04, from https://essd.copernicus.org/articles/9/697/2017/essd-9-697-2017.html (Publisher: Copernicus GmbH) doi: 10.5194/essd-9-697-2017

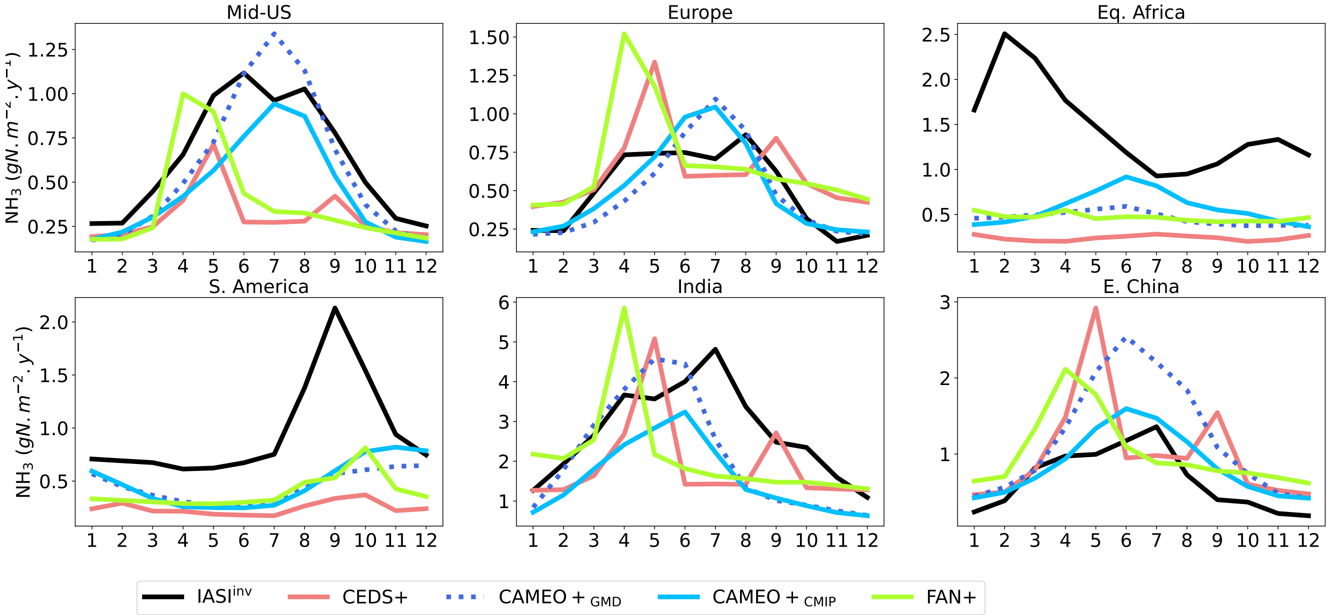

Figure S1. Monthly regional NH3 emissions (gN.m^{-2}.yr^{-1}). The CAMEO emissions from Beaudor et al. (2023) and this study accounting for natural and agricultural emissions aggregated with other sources are represented by the dotted and solid blue lines respectively (CMIP+$_{\mathrm{GMD}}$, CMIP+$_{\mathrm{CMIP}}$). The agricultural sector of CEDS aggregated with other sources is represented by pink solid lines (CEDS+), respectively. The IASI$^{\mathrm{inv}}$ product is shown in black (IASI$^{\mathrm{inv}}$). The agricultural emissions from FANv2 aggregated with other sources are shown in green solid lines (FAN+). Other sources include biomass burning from (van der Werf et al., 2017) and industrial and waste sectors from CEDS (Hoesly et al., 2018). The region boundary coordinates are given as follows in degree : Eq. Africa = [-30N,47N,-14E,18E], Mid-US = [-125N,-75N,20E,50E], Europe = [-15N,40N,35E,60E], S. America = [-70N,-35N,-40E,5E], India = [65N,92N,3E,35E], China = [95N,128N,16E,52E]

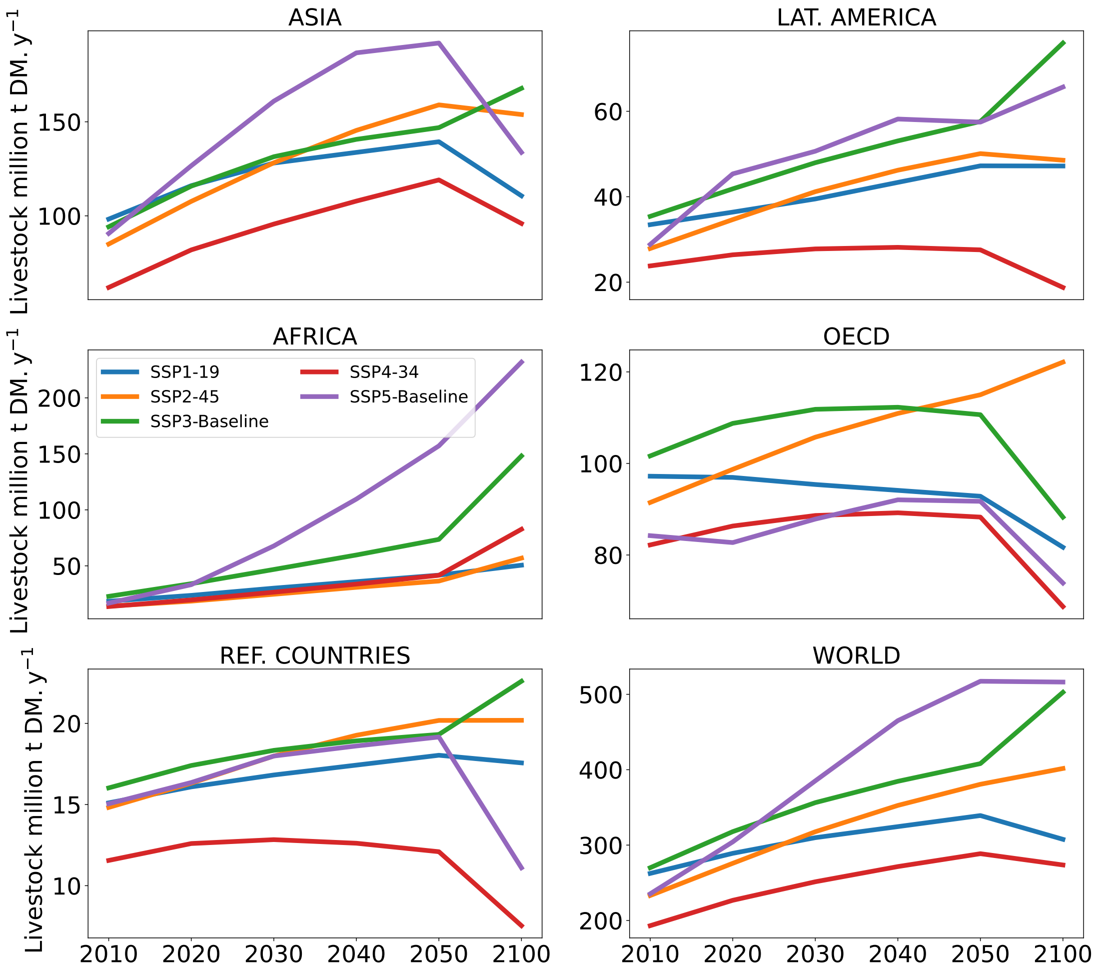

Figure S2. Evolution of the livestock production (million tDM/yr) for the different SSPs of the IAMs framework from 2010 to 2050. SSP5-Baseline here corresponds to SSP5-8.5 used in the text. Data provided in the IIASA database (Riahi et al., 2017).

Regional abbreviations 'REF' accounts for Reforming Economies of Eastern Europe and the Former Soviet Union.

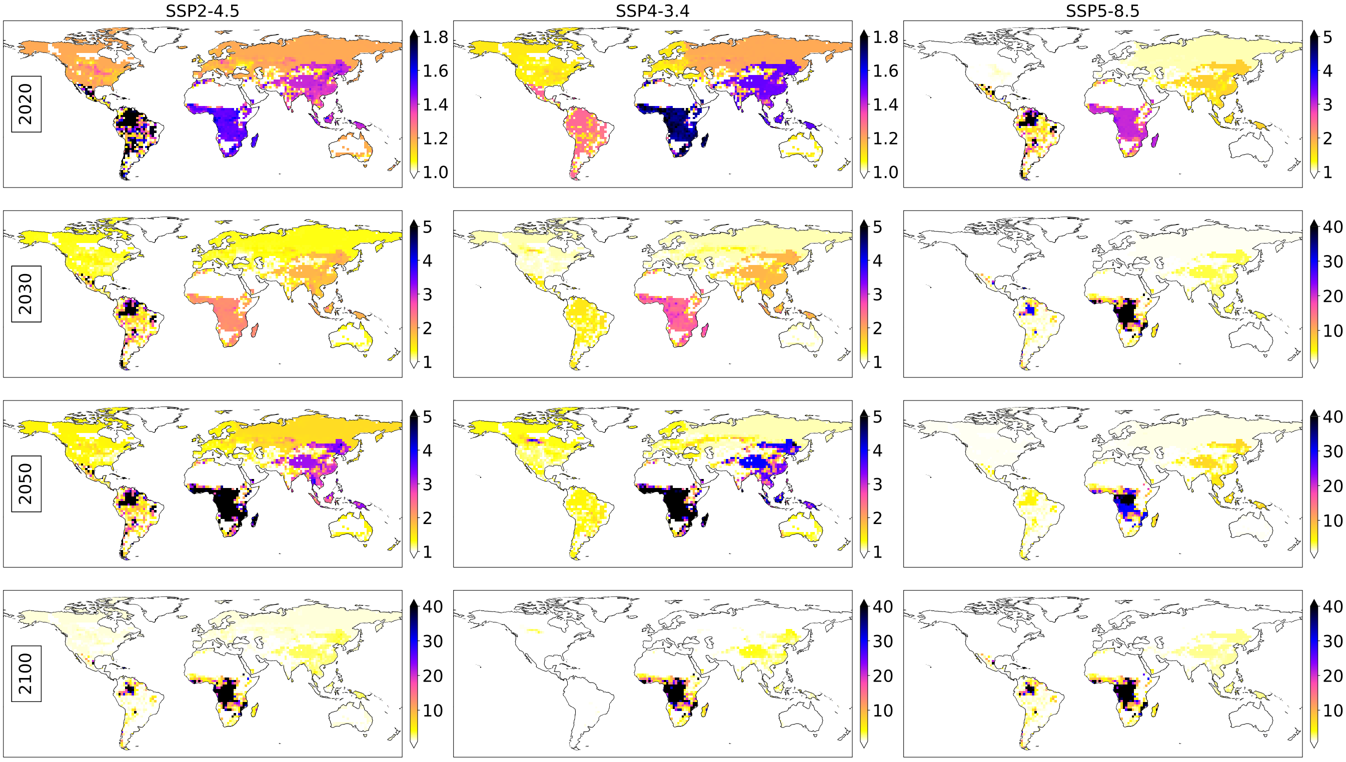

Figure S3. Gridded factors $f_{SSPi(2010\rightarrow y)}$ to obtain the future livestock distributions under the three selected scenarios for year 2020, 2030, 2050 and 2100

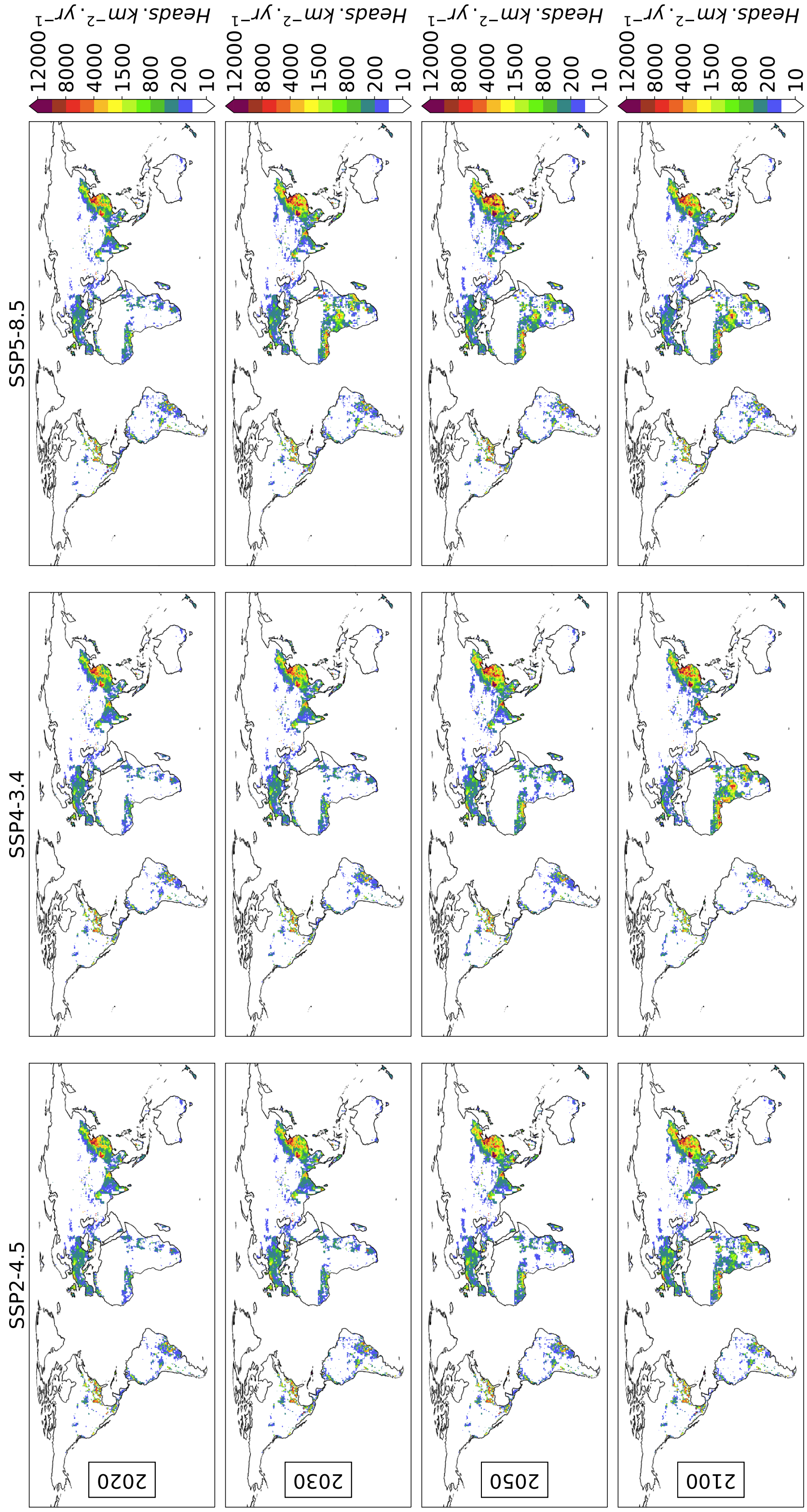

Figure S4. Future livestock distributions under the three selected scenarios for years 2020, 2030, 2050, and 2100 (Heads.km^{-2}.yr^{-1}).

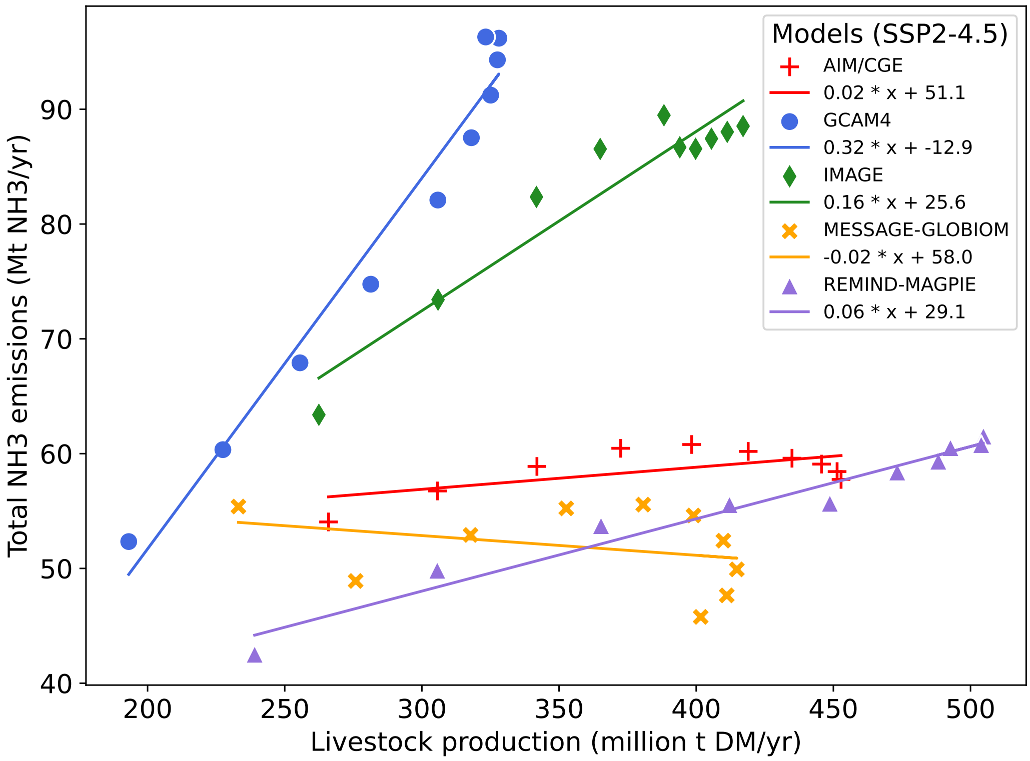

Figure S5. Total (unharmonized) emissions (Mt NH3.yr^{-1}) evolution with livestock production (million t DM.yr^{-1}) simulated by the different IAMs under SSP2-4.5 over 2005-2100. The regression function is indicated in the legend for each model (IIASA database).

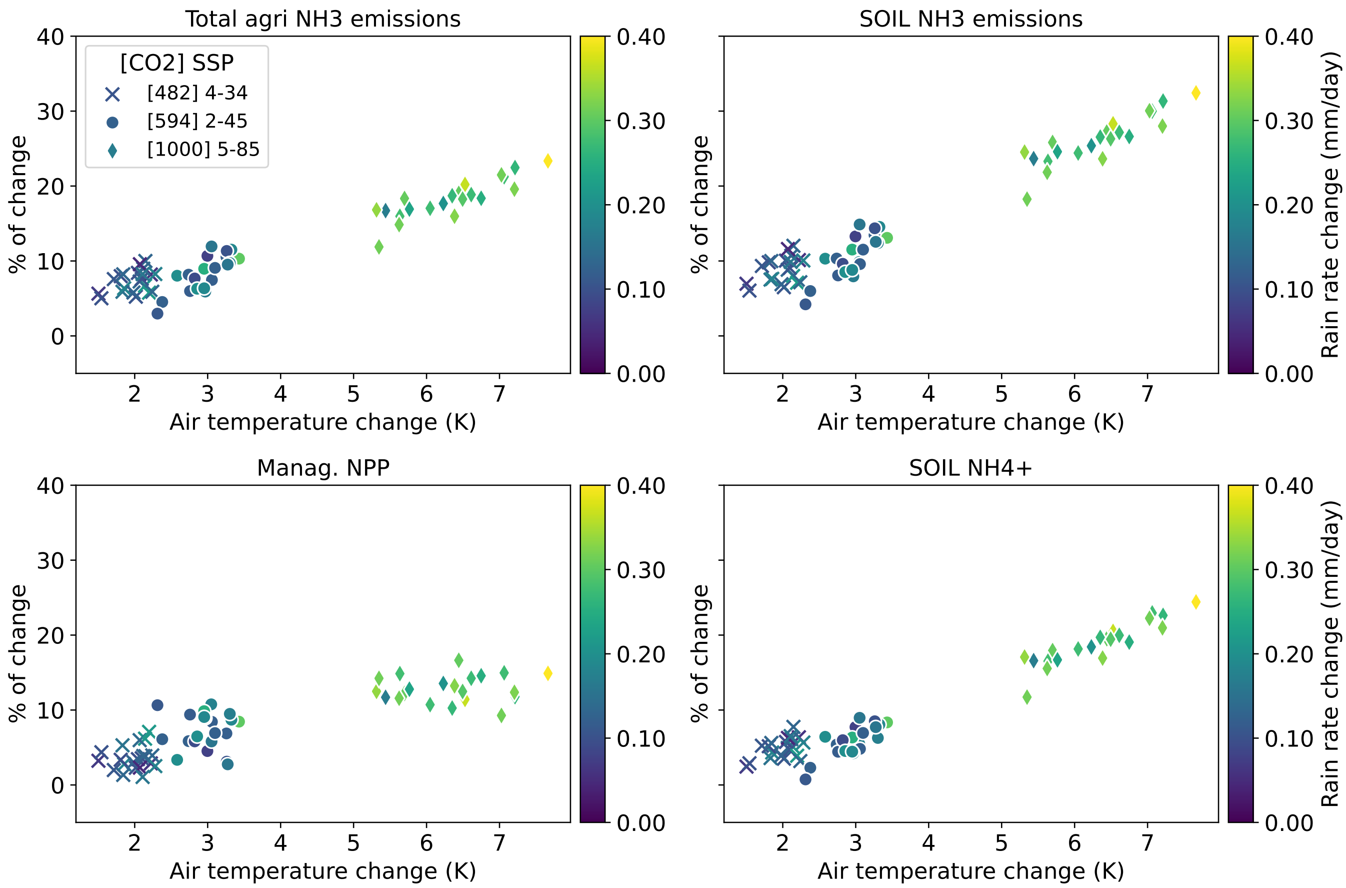

Figure S6. Simulated change in the global mean total agricultural emissions (top left panel), soil emissions (top right panel), grassland and cropland NPP (bottom left), and soil ammonium (bottom right) with temperature and rain rate under the considered SSPs (cross: SSP4-3.4; circle: SSP2-4.5; diamond: SSP5-8.5) for 2080-2100 period. Please note that the different CO_2 levels (in ppm) associated with the SSPs are written into brackets in the legend. The changes are calculated between the simulations where the climate is changing for the future and where the climate is taken for the present day.

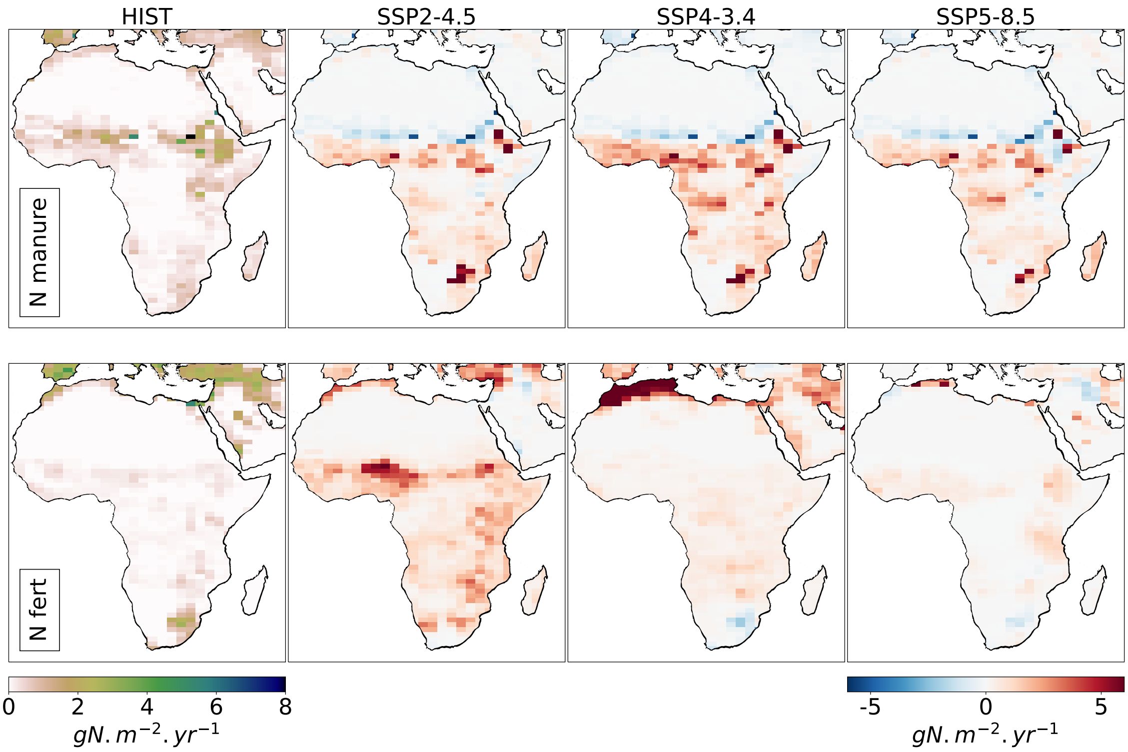

Figure S7. Agricultural N input during the historical period (2005-2014, first column) and absolute differences with the future period (2091-2100) N input under the three SSPs (second, third and last columns) by CAMEO under future climate over Africa (a) and Asia (b). The first row corresponds to the manure applied simulated by CAMEO, and the second row is the fertilizer rate coming from LUH2.Units are in gN.m^{-2}.yr^{-1}.

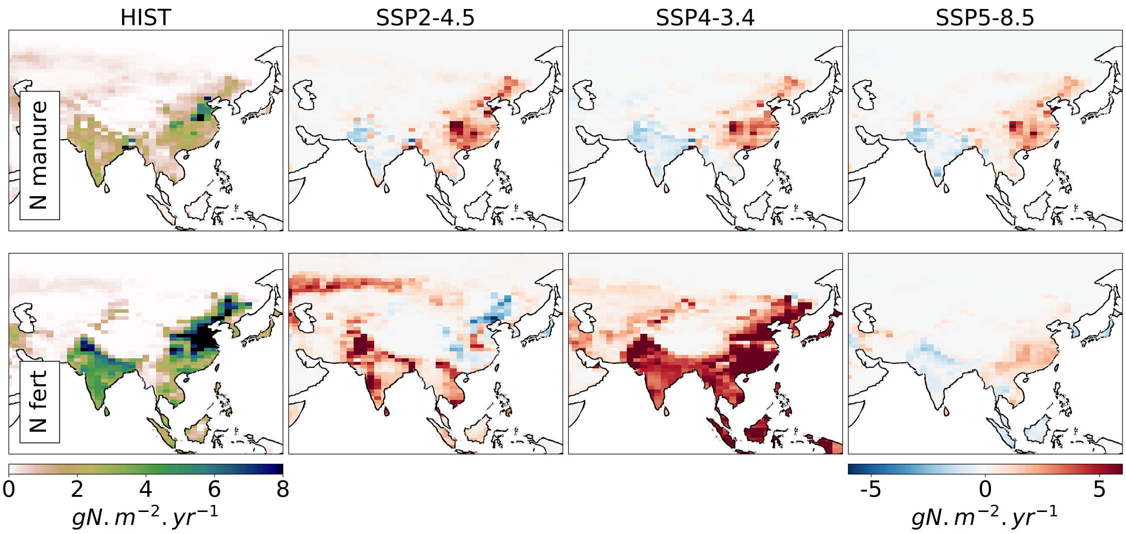

Figure S8. Same as S7.

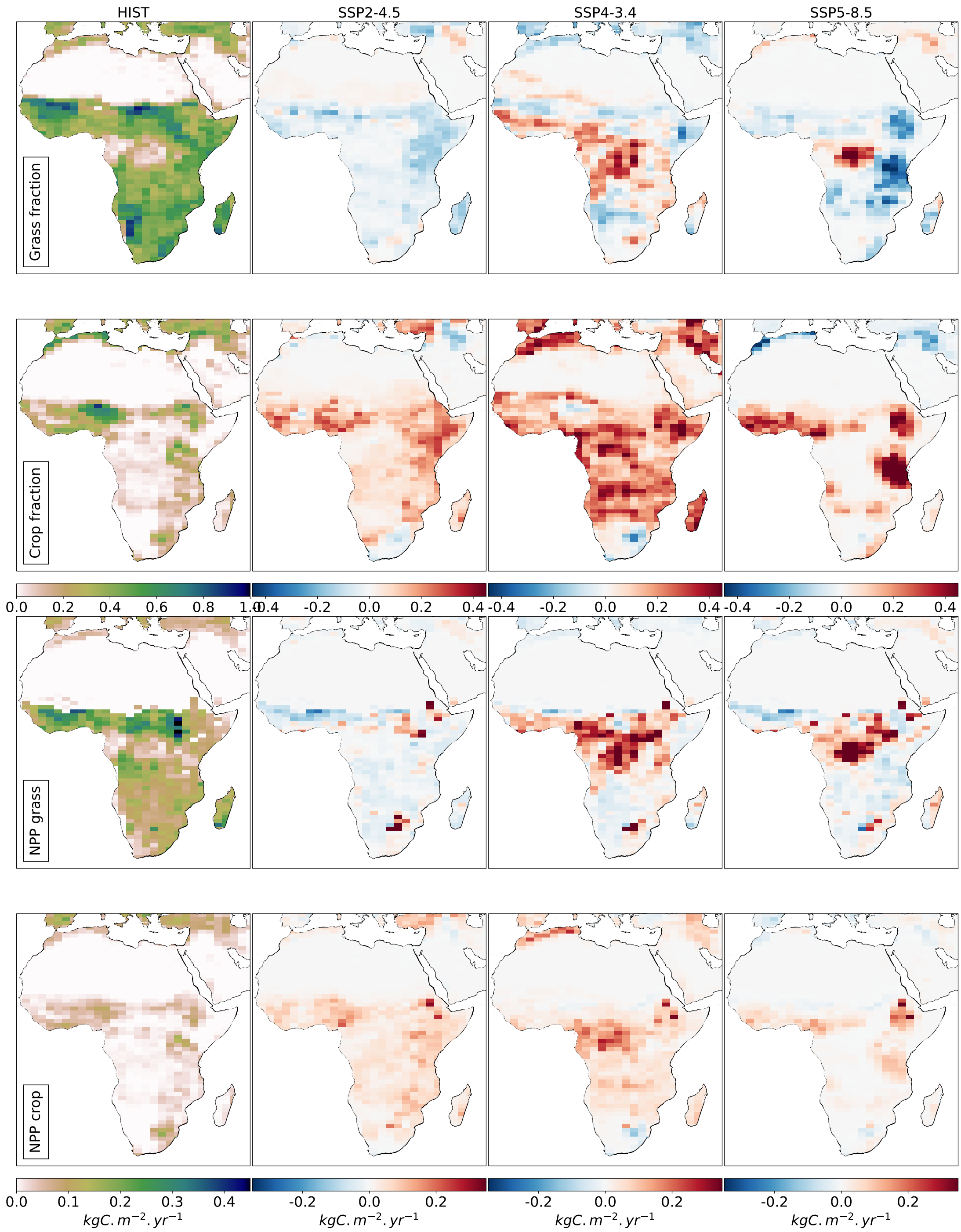

Figure S9. Agricultural Ninput during present-day (2005-2014, first column) and absolute differences with future (2091-2100) Ninput under the three SSPs (second, third and last columns) by CAMEO under future climate. First row corresponds to the manure applied simulated by CAMEO and second row is the fertilizer rate coming from Input4MIP. Units are in gN.m^{-2}.yr^{-1}

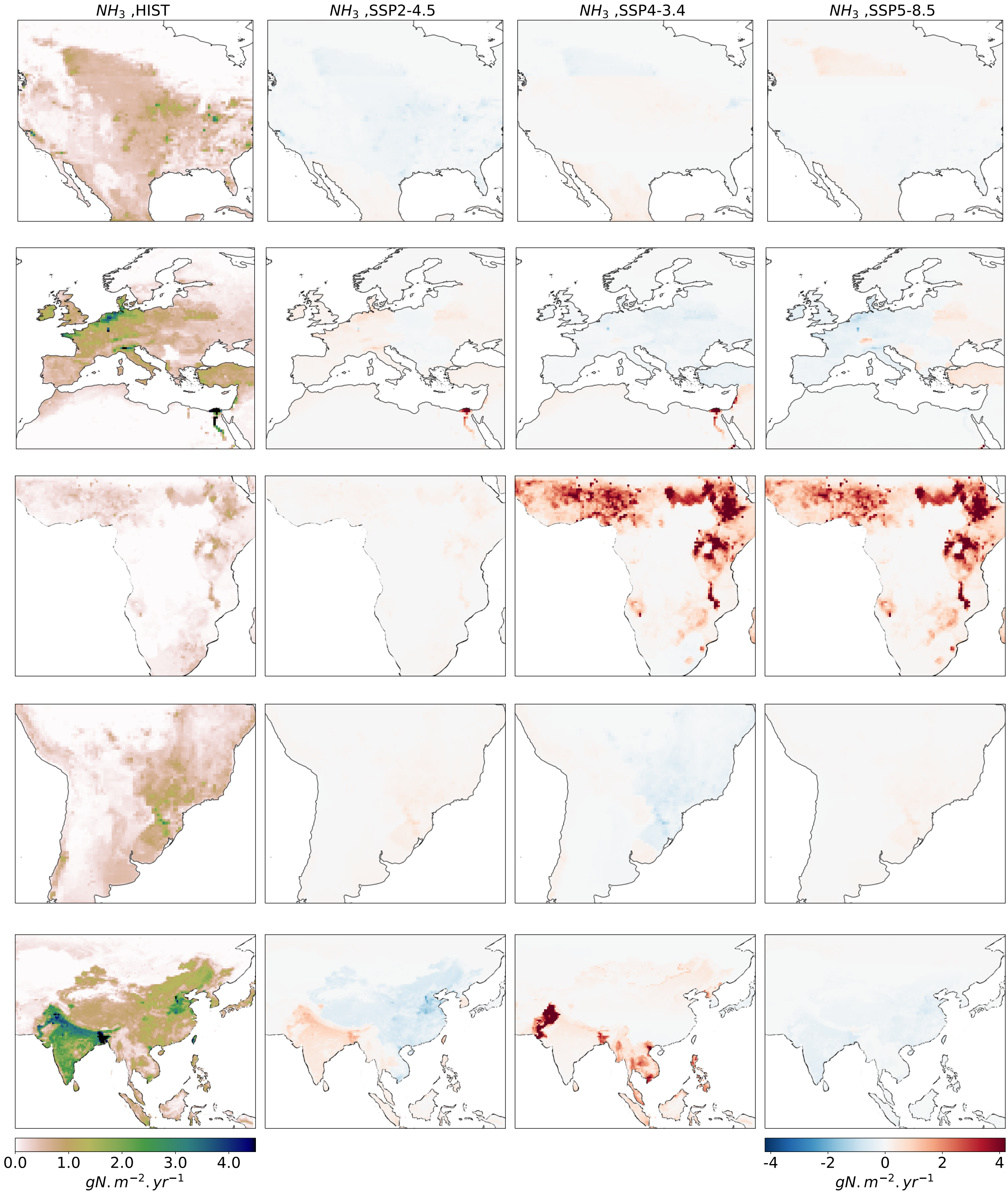

Figure S10. Agricultural emissions in the historical period (2005-2014, first column) and absolute differences between future (2091-2100) and historical emissions under the three SSPs (second, third and last columns) from the harmonized CMIP6 emissions IAMs. Units are in $gN.m^{-2}.yr^{-1}$